Research Journal of Applied Sciences, Engineering and Technology 5(24): 5665-5676, 2013
DOI:10.19026/rjaset.5.4253
ISSN: 2040-7459; e-ISSN: 2040-7467

Submitted: August 03, 2012 Accepted: September 02, 2012 Published: May 30, 2013

Research Article

Reduction of Wind Turbine Torque Fluctuation Using Individual Pitch Control Based on Edgewise Moment

[1]Zhenlan Dou, [1]Simin Peng, [1]Zhibin Ling and [1,2]Xu Cai
[1]Wind Power Research Center, Department of Electronic Information and Electrical Engineering,
[2]State Key Laboratory of Ocean Engineering, Department of Naval Architecture, Ocean and Civil Engineering, Shanghai Jiao Tong University, Shanghai 200240, China

Abstract: In order to eliminate the nonuniform force on the wind rotor caused by wind shear, tower shadow and turbulence and smooth the torque fluctuation of the wind turbine and the unbalanced loads on the wind turbine, a new individual pitch control strategy based on edgewise moment using single neuron PID controller is proposed. That is, the presented control strategy directly controls the blade edgewise moment generated by aerodynamic force. At the same time, to simulate the wind turbine loads, a dynamic model of three-bladed upwind horizontal axis wind turbine is built. Thus, the influence rules of the wind turbine torque fluctuation are deduced at length. Finally, to verify the effectiveness of the proposed individual pitch control system with the single neuron PID controller, the 2MW wind turbine generator system is modeled and simulated. The performance of the controller is illustrated its capability of not only reducing the wind turbine fluctuation, but also smoothing the fluctuation of the flapwise moment, the yaw moment and the tilt moment.

Keywords: Aerodynamic force, edgewise moment, dynamic aerodynamic model, individual pitch control, single neuron PID, wind turbine torque fluctuation

INTRODUCTION

Wind power generation is one of the most mature and well-developed power generation technologies in renewable energy area. In order to enable great role of wind energy in power production, it is necessary to increase the size and the power of wind turbine unit (Hau, 2006; Manwell *et al*., 2002.). With the increasing size of the wind turbine, the turbine is subjected to extreme unbalanced loads because of the uneven distribution caused by wind shear, tower shadow, turbulence and so on Hansen (2008). The unbalanced loads lead to serious damage to the wind turbine, such as blade edgewise vibration, blade flapwise vibration, drive train torsion and tower bending and cause great fatigue loads to the key components of the wind turbine. Moreover, the unbalanced loads will bring many problems to the wind turbine mechanical strength and the power grid quality (Fadaeinedjad *et al*., 2009; Haiyun *et al*., 2010). For large-scale wind turbine with one hundred meter of diameter, these problems are particularly prominent, thus it is necessary to reduce the unbalanced loads on the wind turbine.

The pitch actuator mechanism, regardless of electrical servo or hydraulic servo, usually adopts the Collective Pitch Control strategy (CPC) which the pitch angles of all blades are same. Assuming the wind distribution in the wind rotor plane is uniform without the effects of wind shear, tower shadow and turbulence, the blade pitch angle usually is decided by the effective wind speed or the average wind speed. If every blade of the wind rotor is adjusted by Individual Pitch Control (IPC) according to some certain rules, the forces on blade tend to uniformly in the rotation plane and the amplitudes of the blade root moments in two directions reduce in different degrees according to the theoretical aerodynamic analysis. Moreover, the fluctuation of the wind turbine torque and the unbalance loads reduce.

Recently, the studies of IPC mainly focuses on cyclic pitch control, D-Q axis transformation IPC, Coleman transformation IPC, weight coefficient distribution IPC, the smart rotor control and so on. The first cyclic pitch control is a compensation control using aerodynamic force generated by cycle pitch change based on the measured tilt moment and yaw moment (Lescher *et al.*, 2005; Markou *et al.*, 2011). The second D-Q axis transformation IPC is to control the load components, which come from the measured blade root loads by the D-Q axis transformation (Bossanyi, 2003, 2005; Liu *et al.*, 2006; Jelavic *et al.*, 2008; Wilson *et al.*, 2009). Assuming there is no interaction between the orthogonal coordinate axes, the classical control method for single input single output can used to

Corresponding Author: Zhenlan Dou, Wind Power Research Center, Department of Electronic Information and Electrical Engineering, Shanghai Jiao Tong University, Shanghai 200240, China

control the load components. The third Coleman transformation IPC is the wind turbine multivariable control, which the pitch control loop is decoupled into three independent linear time-invariant feedback control loops by the Coleman transformation. The three independent control loops are the control loop of wind rotor speed, the yaw control loop and the tilt control loop respectively (Geyler and Caselitz, 2007; Kanev and Van, 2010; Selvam *et al.*, 2009; Van, 2006). The forth weight coefficient distribution IPC is the pitch angle adjusted by the dynamic weight coefficient along with the aerodynamic force change (Trudnowski and LeMieux, 2002). The last smart rotor control is to adopt a new-type rotor whose blade are equipped with a number of control devices that locally change the lift profile on the blade and combined with appropriate sensors and controllers (Barlas *et al.*, 2006; Lackner and Van Kuik, 2010). Because MW-scale Wind Turbine Generator System (WTGS) are grid-connected, the torque fluctuation of wind turbine easily results in many problems, such as the fluctuant power output of WTGS and the poor power grid quality. However, the above IPC strategies mainly focus on the reduction of the blade flapwise moment or improving the blade structure without considering the torque fluctuation of wind turbine or the blade edgewise moment.

In this study, to reduce the wind turbine torque fluctuation, a novel control strategy using IPC based on edgewise moment is proposed. Moreover, the single neuron PID controller is used to IPC. This controller adjust the pitch angle individually according to the measured blade edgewise moment and the ideal reference edgewise moment calculated by the effective wind speed without taking into account of any influenced factors. Furthermore, the fluctuation rules of the wind turbine torque are deduced in details based on the dynamic wind turbine model. Finally, to verify the effectiveness of the proposed IPC with single neuron PID controller, the model of a 2MW WTGS is set up. The simulation results show that this proposed IPC system with single neuron PID controller can not only directly smooth the fluctuation of wind turbine torque and the blade edgewise moment, but also indirectly reduce the fluctuations of the blade flapwise moment, the yaw moment and the tilt moment. These provide certain guiding significance to the IPC implementation in wind field.

The analysis of loads on the blade and the torque fluctuation of the wind turbine: Because the mechanical energy is converted from the kinetic energy of wind by the wind rotor, the loads on the turbine, the tower and the hub come from the external loads on the blade (Li *et al.*, 2004). The blade loads are aerodynamic, gravity, inertia and so on.

The total edgewise moment of a single blade is mainly composed of the edgewise moment generated by aerodynamic force on the blade and the edgewise moment generated by the blade gravity according to the aerodynamic theory, the other blade loads are so small that they are neglected. That is:

$$M_{Edgewise,i} = M_{Gravity,i} + M_{Edge,i} \quad (1)$$

where,

$M_{Edgewise,\ i}$ = The blade i-th total edgewise moment
$M_{Gravity,\ i}$ = The blade i-th gravity moment
$M_{Edge,\ i}$ = The blade i-th edgewise moment generated by the aerodynamic force

For the three-bladed upwind horizontal axis wind turbine, the wind turbine torque is the sum of the edgewise moment from three blades:

$$M_{Turbine} = \sum_{i=1}^{3} M_{Edgewise,i} \quad (2)$$

$$\sum_{i=1}^{3} M_{Gravity,i} = 0 \quad (3)$$

where, $M_{Trubine}$ is the wind turbine torque.

The other aerodynamic load on the blade is the flapwise moment and the vector sum of $M_{flapwise,\ i}$ are yaw moment and tilt moment respectively:

$$M_{yaw} = \sum_{i=1}^{3} M_{Flapwise,i} \sin(\phi_i) \quad (4)$$

$$M_{tilt} = \sum_{i=1}^{3} M_{Flapwise,i} \cos(\phi_i) \quad (5)$$

where,

$M_{flapwise,\ i}$ = The blade i-th root flap wise moment
ϕ_i = The blade i-th azimuth
M_{yaw} = The yaw moment on the tower
M_{tilt} = The tilt moment on the tower

Take the blade of 2 MW wind turbine as an example, the loads on the blade 1 are calculated based on the element theory according to the blade geometry parameters, the blade aerofoil parameters, the blade mass and the blade stiffness parameters. The relationship among $M_{Edgewise,\ 1}$, $M_{Edge,\ 1}$ and $M_{gravity,\ 1}$ is shown in Fig. 1. Although the edgewise moment component caused by the aerodynamic force is significantly less than the edgewise moment component caused by the gravity, the former moment is the main influencing factor and cannot be neglected.

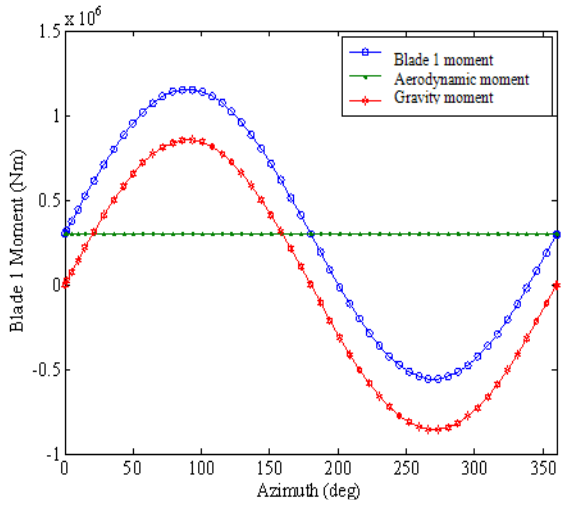

Fig. 1: Relationship diagram of the loads on the blade 1

By analyzing the aerodynamic loads on the wind turbine, the blade edgewise moment generated by aerodynamic force on the blade is the main fluctuation factor of the wind turbine torque and the wind turbine power output. In addition, the fluctuations of the yaw moment and the tilt moment derive from are the blade flapwise moment. If the edgewise moment on the blade is controlled by the IPC strategy, the wind turbine torque fluctuation is directly reduced and the wind turbine power output remains stable.

Dynamic wind turbine aerodynamic model for IPC: In order to analyze the operation principle of the IPC, the loads on the wind rotor and the blade influenced by wind shear, tower shadow and turbulence should be simulated. The traditional model of the wind turbine is built based on the known wind turbine torque coefficient. Because the pitch angle and its impact

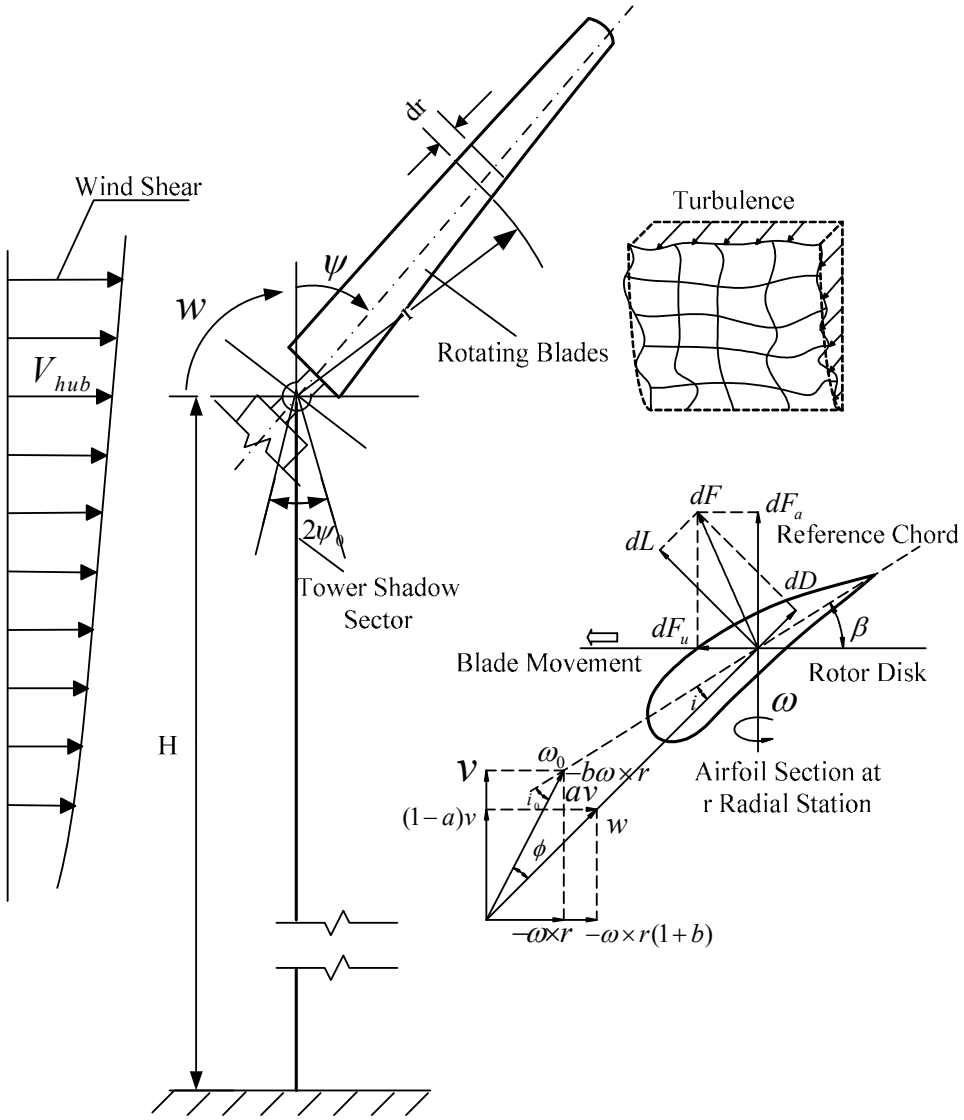

Fig. 2: Diagram of force analysis and speed vector of blade element

on the wind turbine aerodynamic torque are coupled, the pitch angle influences on the lift force and the drag force on the blade cannot be analyzed separately (Abdin and Xu, 2000). In order to implement the IPC strategy, the built wind turbine model can calculate the aerodynamic force and the corresponding loads on the blade element.

The aerodynamic force dF on the blade element dr generate from the action of the airflow with the speed of w. The dF can be decomposed into the dL and dD along with the direction of vertical and parallel to the relative speed and it also can be decomposed into the dF_a and dF_u along the direction of vertical and parallel to the rotating plane, which are shown in Fig. 2. The edgewise moment and the flapwise moment on the blade element derive from the dF_u and the dF_a, respectively.

$$dF_a = dL\cos I + dD\sin I = \frac{1}{2}\rho w^2 l dr(C_l\cos I + C_d\sin I) \quad (6)$$

$$dF_u = dL\sin I - dD\cos I = \frac{1}{2}\rho w^2 l dr(C_l\sin I - C_d\cos I) \quad (7)$$

where,

C_l = The lift coefficient of the blade element
C_d = The drag coefficient of the blade element
l = The chord length of the blade element
I = The flow angle, which can be expressed as $I = \beta + i$

Because the diameter of the MW-level wind turbine is usually up to hundred of meters, there is a great difference between the torque at the blade tip element and the torque at the blade root element, as in (Dou *et al.*, 2011). Considering that the number of blade elements cannot increase without limitation, the number of the blade element is re-optimized by the weight coefficient assignment. Assuming the total number of blade element is p, the blade elements is divided into n feature regions according to the parameters variation of the airfoil and the number of the blade element distributed in each region is determined by the weight coefficient k_t, that is:

$$p_t = k_t \times p \quad (8)$$

where, $\sum_{t=1}^{n} k_t = 1$

The aerodynamic loads on the blade are calculated by integrating the whole blade.

$$F_a = \frac{1}{2}\int_{r_0}^{R}\rho w^2 l(C_l\cos I + C_d\sin I)dr \quad (9)$$

$$F_u = \frac{1}{2}\int_{r_0}^{R}\rho w^2 l(C_l\sin I - C_d\cos I)dr \quad (10)$$

$$M_{Edge} = \frac{1}{2}\int_{r_0}^{R}\rho w^2 l(C_l\sin I - C_d\cos I)rdr \quad (11)$$

$$M_{Flapwise} = \frac{1}{2}\int_{r_0}^{R}\rho w^2 l(C_l\cos I + C_d\sin I)rdr \quad (12)$$

where,

r_0 = The radius of the hub
R = The radius of the blade
F_a = The axial force on the blade
F_u = The lateral force on the blade
M_{Edge} = The edgewise moment on the blade
$M_{flapwise}$ = The flap wise moment on the blade

In order to simple realize and accurate calculation, the blade dr is equivalent to the Δr variation and the length of blade element chord is the average length of both ends of this segment.

The aerodynamic model simulates the wind speed of the blade tip, the wind turbine torque, the loads on the blade 1 and the loads on the tower underling the wind, as shown in Fig. 3. The turbulence intensity of wind is 0.15, the wind shear coefficient is 0.2 and the average wind speed is 12 m/s. Considering the effects of the wind shear, the tower shadow and the turbulence, the wind speed of the blade tip is relative maximum when the blade rotates to the top of the wind rotor plane, but the wind speed is relative minimum when the blade 1 rotates to the bottom of the wind rotor plane, as shown in Fig. 3a. Considering none of the influence factors, the wind speed distribution is uniform, the wind turbine torque and the loads on the blade 1 are constant and the yaw moment and the tilt moment on the tower are zero (Normal curve), as shown in Fig. 3b-3f. Considering only the wind shear effect, the edgewise moment and the flapwise on the blade 1 are minimum when the blade 1 rotates to the bottom of the wind rotor plane. The edgewise moment and the flapwise on the blade 1 are maximum when the blade 1 rotates to the top of the wind rotor plane, as shown in Fig. 3c and 3d. Considering the effect of the tower shadow, the wind speed decrease rapidly when the blade 1 rotates into the tower shadow region and the edgewise moment and the flapwise on the blade 1 decrease with the wind speed. Considering the wind shear effect and the tower shadow effect, the loads fluctuation on the blade 1 are maximum compared with the wind shear effect or the tower shadow effect. Considering the effect of the wind shear, the tower shadow and the turbulence, the general change of the loads on blade 1 is consistent with the loads fluctuation affected by wind shear and tower shadow. In addition, the fluctuations of the wind turbine torque, the yaw moment and the tilt moment are proportional to the wind speed variation, as shown in Fig. 3b-f. The amplitude of torque fluctuation caused by the tower shadow is 5.85% compared with the rated wind turbine torque (Normal curve). The amplitude of

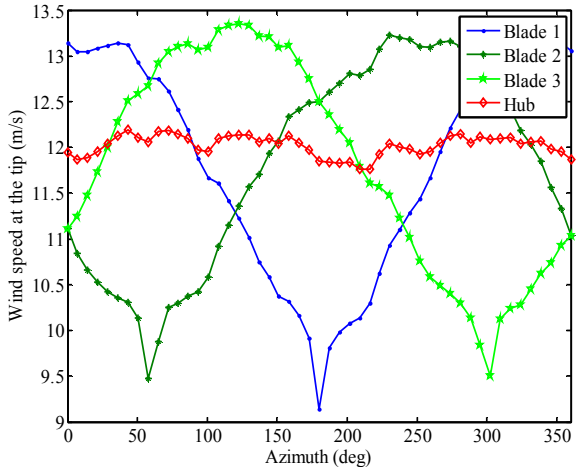

(a) The wind speed at the blade tip

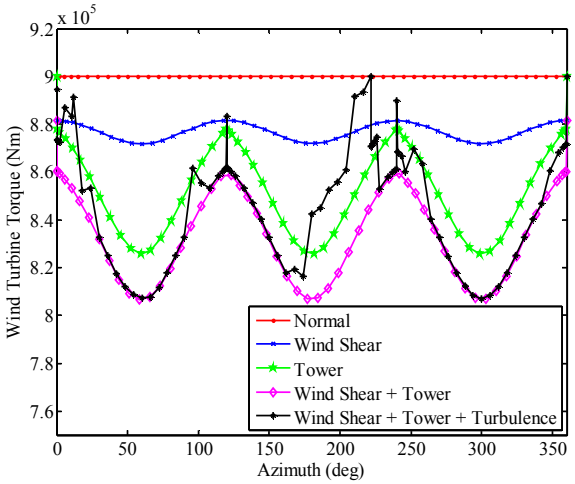

(b) The wind turbine torque

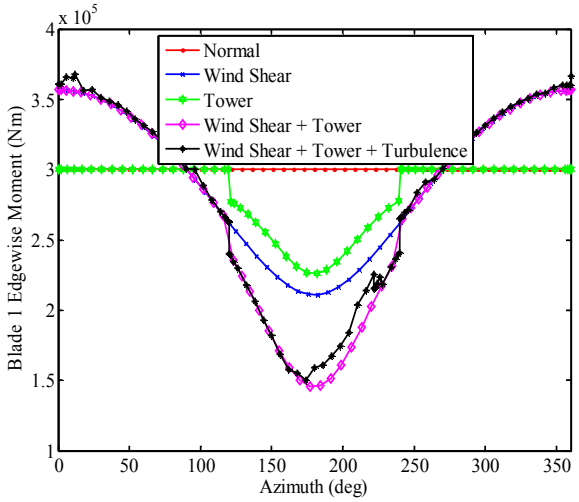

(c) The edgewise moment on the blade 1

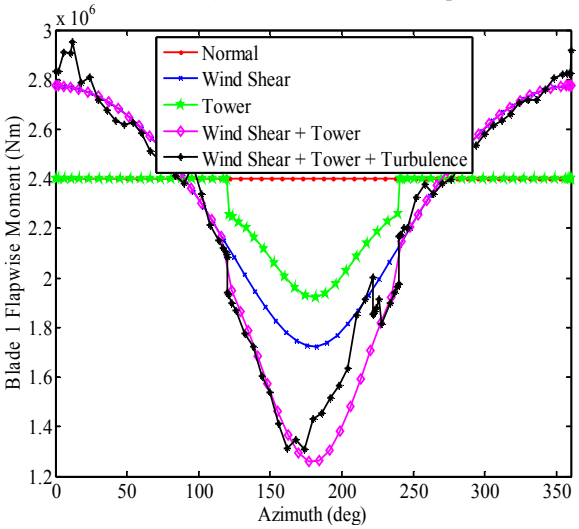

(d) The flap wise moment on the blade 1

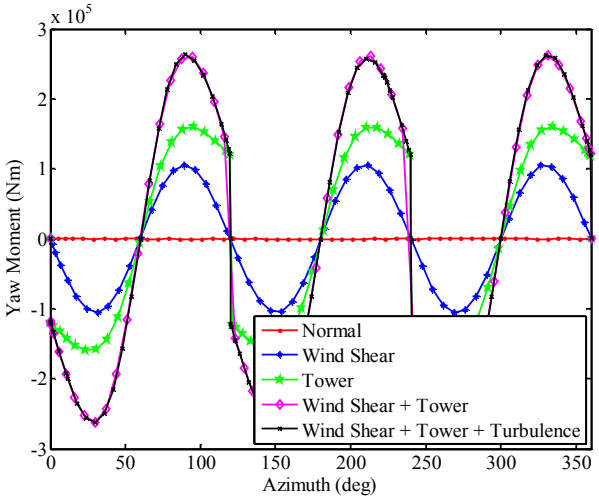

(e) The yaw moment on the tower

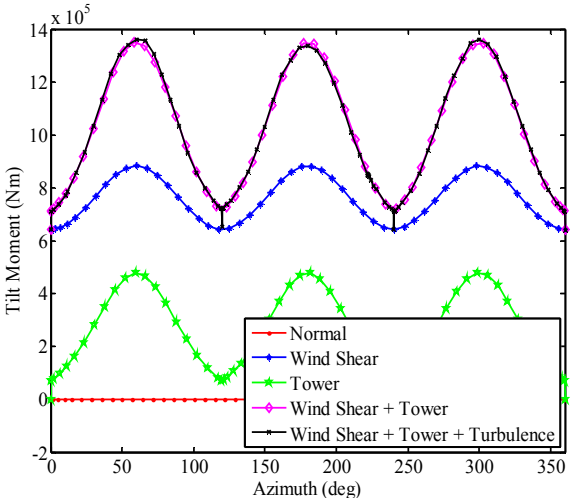

(f) The tilt moment on the tower

Fig. 3: Loads on the wind turbine

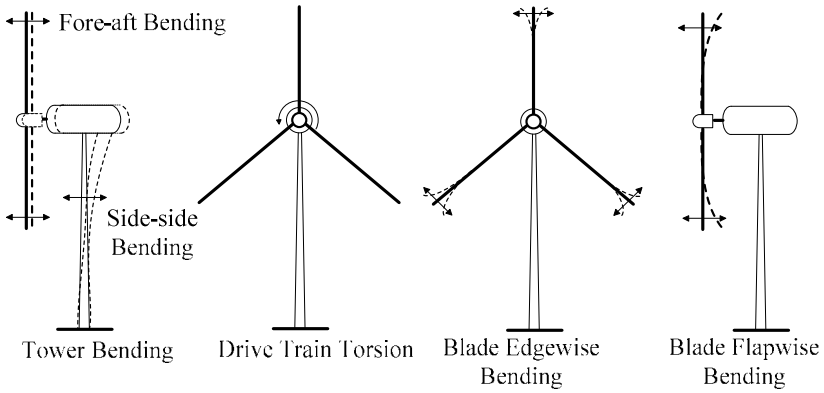

Fig. 4: Non uniform forces on the wind turbine

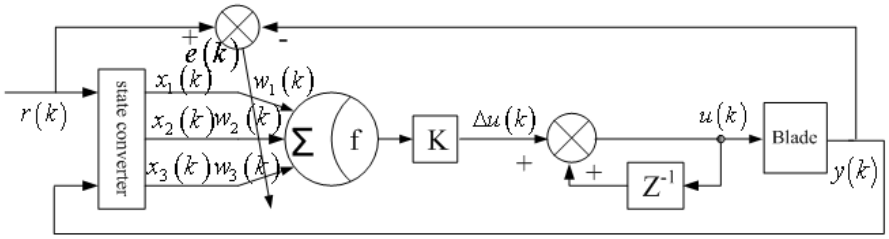

Fig. 5: Structure of SNPID controller

torque fluctuation caused by wind shear is 1.1% .In addition, the amplitude of torque fluctuation caused by the tower shadow and the wind shear is 6%. Furthermore, the amplitude of torque fluctuation caused by turbulence relates to the intensity of the turbulence and the scale of the turbulence. From the Fig. 3b-3f, the wind shear and the tower shadow cause the 1 times frequency (1P) fluctuation of the edgewise moment and 1P fluctuation of the flapwise moment on the blade and result in 3 times frequency (3P) fluctuations of the wind turbine torque, the yaw moment and the tilt moment on the tower.

Reduction of torque fluctuation by individual pitch control in WTGS: Wind shear, tower shadow and turbulence cause the nonuniform forces such as tower bending, drive train torsion, blade edgewise bending and blade flap wise bending of wind turbine, as shown in Fig. 4.

Under the premise of the maximum wind power captured, the IPC control target is to eliminate the unbalanced loads as much as possible. When the wind rotor speed is equal to the rated rotor speed, the variation of pitch angle according to some certain rules (IPC) can result in the attack angle change of the blade. Because the change of attack angle causes the changes of the normal force coefficient and the lateral force coefficient, the forces on blade tend to uniformly in the rotation plane. Moreover, the aerodynamic loads on the blade reduce greatly and the wind turbine torque keeps stable. Because of the nonlinearity and complexity of the loads and the pitch angle according to the analysis of wind rotor loads, it is difficult to control by a conventional controller. A Single Neuron self-adaptive PID (SNPID) controller has adaptive and self-learning ability, which not only calculate easily with the simple structure, but also can adapt the environment change with strong robustness (Wu *et al*., 2008; Zhao and Yang, 2008). Therefore, the SNPID-IPC can be used to adjust the blade pitch angle to reduce the edgewise moment fluctuation of blade. The structure of the controller is shown in Fig. 5, where, r (k), y (k) is state convert input, x_1, x_2, x_3 are the state convert outputs which have the following relationship.

$$\begin{aligned} x_1(k) &= r(k) - y(k) = e(k) \\ x_2(k) &= \Delta e(k) = e(k) - e(k-1) \\ x_3(k) &= \Delta^2 e(k) = e(k) - 2e(k-1) + e(k-2) \\ u(k) &= u(k-1) + K\sum_{i=1}^{3} w_i(k) x_i(k) \end{aligned} \tag{13}$$

where,

K = The single neuron proportional coefficient
$w_i(k)$ = The weight coefficient of corresponding to $x_i(k)$
$u(k)$ = The output of the SNPID controller

The functions of self-adaptive and self-organization of SNPID controller is implemented by adjusting the weight coefficient. In addition, the adjustment of weight coefficient realizes according to a rule of supervised Hebb learning. In order to guarantee the convergence of learning algorithm and the robustness of the control strategy, the weight coefficients should normalized. Compared to the traditional PID controller, the $w_1(k)$, $w_2(k)$, $w_3(k)$ is equivalent to the integral, proportional and differential item of the traditional controller, respectively.

$$w_i'(k) = w_i(k) \Big/ \sum_{i=1}^{3} w_i(k) \tag{14}$$

$$\begin{aligned} w_1(k) &= w_1(k-1) + \eta_I e(k)u(k)x_1(k) \\ w_2(k) &= w_2(k-1) + \eta_P e(k)u(k)x_2(k) \\ w_3(k) &= w_3(k-1) + \eta_D e(k)u(k)x_3(k) \end{aligned} \tag{15}$$

where, η_I, η_P and η_D are the rate of integration, proportional and differentiation respectively.
Then the output of SNPID is as the following.

$$u(k) = u(k-1) + K\sum_{i=1}^{3} w_i'(k)x_i(k) \tag{16}$$

The on-line learning of the parameters of PID are mainly related to e(k) e(k-1) z(k). So the corrected algorithm of weight coefficients for single neural self-adaptive PID controller are modified, which $x_i(k)$ is changed as e(k) + Δe(k), Δe(k) = e(k) – e(k–1) and z(k) = e(k).

The input of the SNPID-IPC controller is the difference between the ideal blade edgewise moment and the actual blade edgewise moment generated by the aerodynamic force. And the output of the controller is the deviation of pitch angle, that is, the blade pitch angle is the collective pitch angle minus the deviation of pitch angle. The initial value of SNPID-IPC controller are $w_1 = 0.0067$, $w_2 = 0.007$ and $w_3 = 0.0001$, ,the rate of learning is η_I 0.15×10^{-4}, $\eta_P = 0.3\times10^{-2}$, $\eta_D = 0.15\times10^{-5}$ and the proportional coefficient of the single neuron is K = 0.3.

SIMULATION RESULT AND ANALYSIS

In this study, in order to verify the effectiveness of IPC with SNPID controller, a typical 2 MW three-blade upwind horizontal axis wind turbine is modeled and simulated with various wind conditions: a ramp wind speed and a turbulence wind speed. The parameters of the wind turbine are as shown in Table 1.

Figure 6 illustrates the blade root moments using CPC. The wind speed at the hub is a ramp wind speed as shown in Fig. 6a. Considering the effects of wind shear and tower shadow, the edgewise moment and the flapwise moment on the three blades using CPC are shown in Fig. 6b and 6c. As the difference of the adjacent blade positions is 120 deg, the phase of the edgewise moment and the flapwise moment of the adjacent blades are also equal to 120 deg. With the increasing of wind speed, the edgewise moment fluctuation increases, but the average edgewise moment

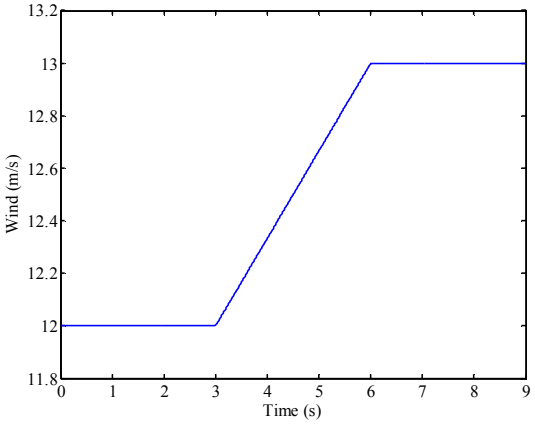

(a) The wind speed at the hub

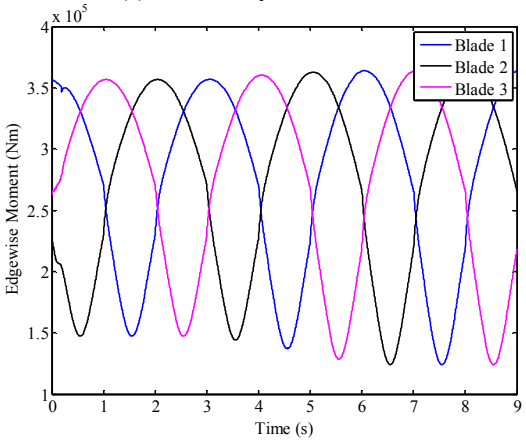

(b) The edgewise moment on the blade

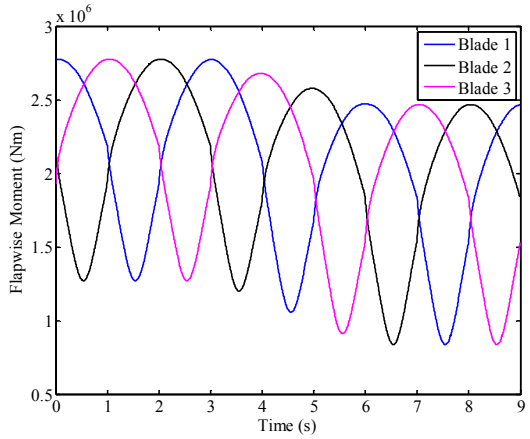

(c) The flap wise moment on the blade

Fig. 6: Blade root moments using CPC

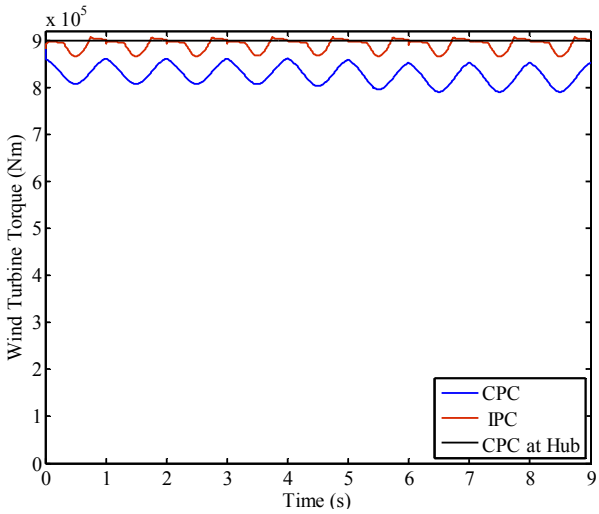

(a) The wind turbine torque

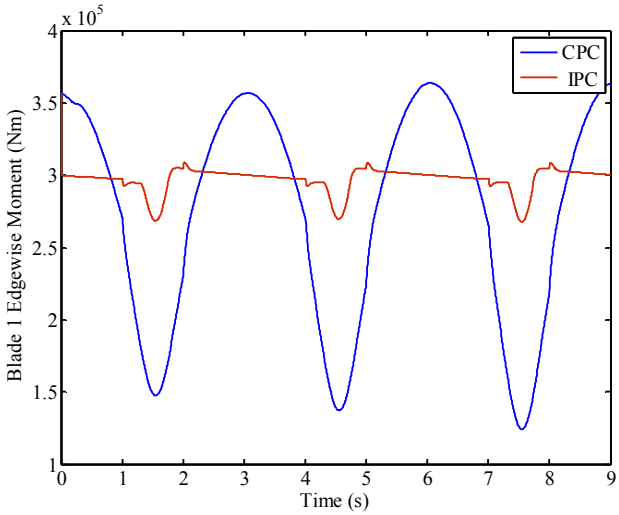

(b) The edgewise moment on the blade 1

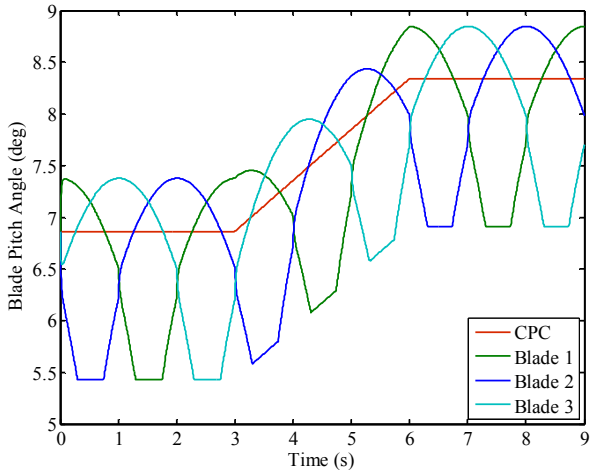

(c) The pitch angle of three Blades

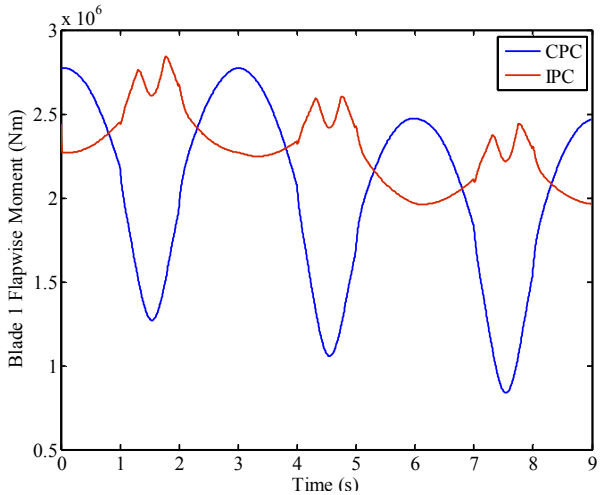

(d) The flap wise moment on the blade 1

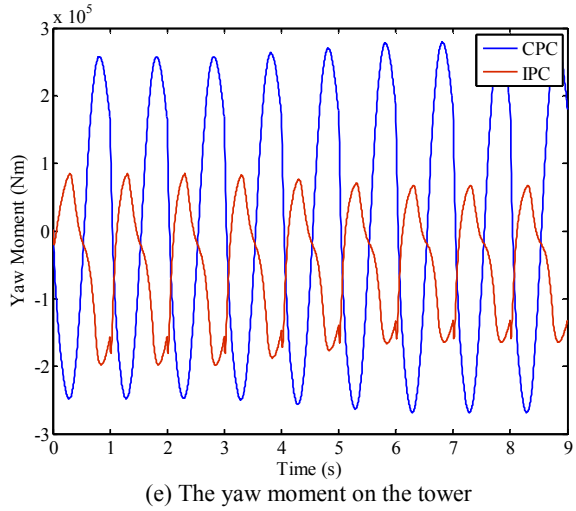

(e) The yaw moment on the tower

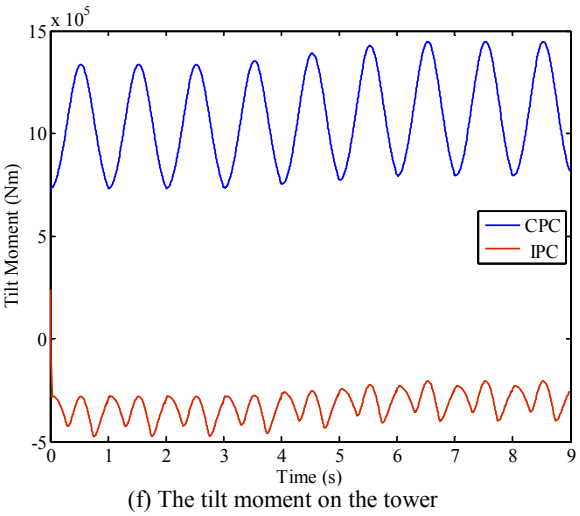

(f) The tilt moment on the tower

Fig. 7: Control effect diagram using IPC with the ramp wind

Table. 1: Wind turbine parameters

Rated power	2 MW
Rated wind rotor speed	21 r/min
Wind rotor diameter	80 m
Hub radius	1.5 m
Hub height	61.5 m
Tower radius	1.75 m
Rotor overhang	3.7 m
Rated wind speed	9.9 m/s
Cut in wind speed	4 m/s
Cut out wind speed	25 m/s
Wind shear exponent	0.2

is unchanged. In addition, though the average flapwise moment decreases, the flapwise moment fluctuation is 10 times as much as the edgewise moment fluctuation.

- **Wind regime 1: a ramp wind:** Figure 7 illustrates the response of the system using IPC underling the ramp wind speed. The variable of the wind at the hub is as shown in Fig. 6a and 7a illustrates the wind turbine torque (CPC at Hub curve) keeps as the rated wind turbine torque when the wind speed distributes uniformly in the rotating plane. Considering the effects of wind shear and tower shadow, the wind turbine fluctuation (CPC curve) decreases in a small level (about 6%) compared to the rated wind turbine torque. In addition, the upper and lower fluctuation of the wind turbine torque is about 10% compared to the rated torque. After using the IPC with SNPID controller, the wind torque fluctuation (IPC curve) decreases greatly to 2.5% compared to the rated torque and the wind torque tends to the rated wind turbine torque, which maintains the generator output power unchanged.

Figure 7b illustrates the fluctuation of the edgewise moment on the blade 1 reduces directly by the IPC compared to the CPC. Because the wind turbine torque is the sum of the edgewise moments on the three blades and the phase of the edgewise moments on the two adjacent blades is equal to 120 deg, the variable of the blade1 edgewise moment is the same as some parts of the wind turbine torque fluctuation. In addition, the moment fluctuation of the blade 2 and the blade 3 is similar with the blade 1.

Figure 7c demonstrates the collective pitch angle changes (CPC curve) with the wind speed. The blade pitch angle not only relates to the wind speed, but also relates to the blade position in the rotating plane. When the blade rotates from the top position to the bottom position in the rotating plane, the pitch angle decreases; and when the blade rotates from the bottom position to the top position, the pitch angle increases. Meanwhile, the pitch angle phase of the adjacent blades (Blade i curve) keeps at 120 deg as the azimuth difference of two adjacent blades is 120 deg.

Furthermore, the flapwise moment fluctuation, the yaw moment fluctuation and the tilt moment fluctuation reduce significantly by individual pitch indirect control with SNPID controller compared to the CPC, as shown in Fig. 7d-7f.

These results indicate this IPC with SNPID controller not only smoothes the fluctuation of wind turbine torque, but also weakens the other loads on the blade. Therefore, this IPC has obvious advantages compared with the traditional CPC.

- **Wind regime 2: a turbulence wind:** Figure 8 illustrates the response of the system using IPC underling a turbulence wind. Figure 8a shows the variation of the wind speed at the hub. Figure 8b-8f demonstrates the changes of the loads (CPC curve) are in accord with the variable of the turbulence wind. Figure 8b shows the wind turbine torque (IPC curve) is close to the rated wind turbine torque (CPC at Hub curve) and the fluctuation becomes small compared to the CPC. In addition, the Fig. 8c-8f illustrate the loads (IPC curve) are reduced effectively by individual pitch indirect control with the SNPID controller comparing with the CPC.

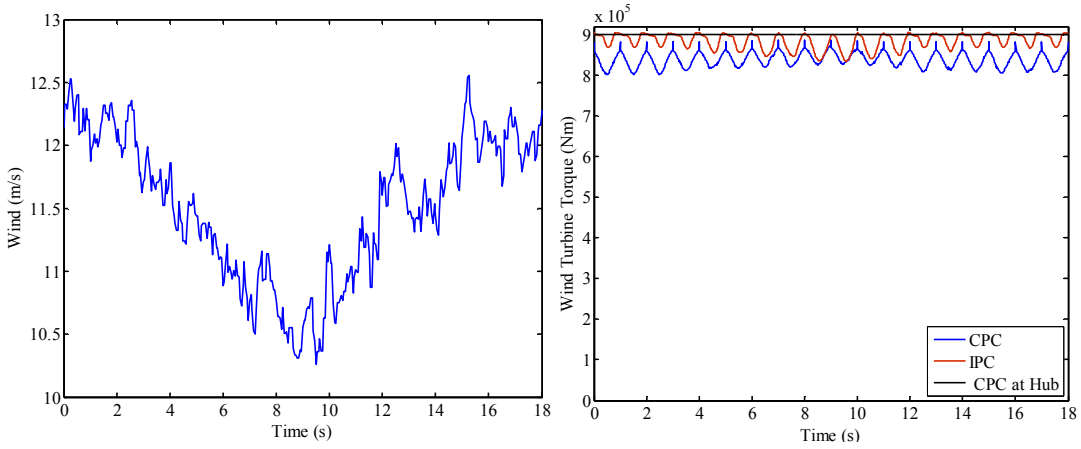

(a) The wind speed at the hub

(b) The wind turbine torque

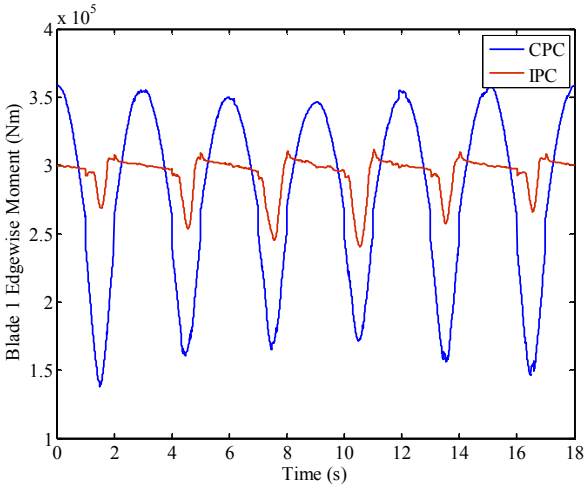

(c) The edgewise moment on the blade 1

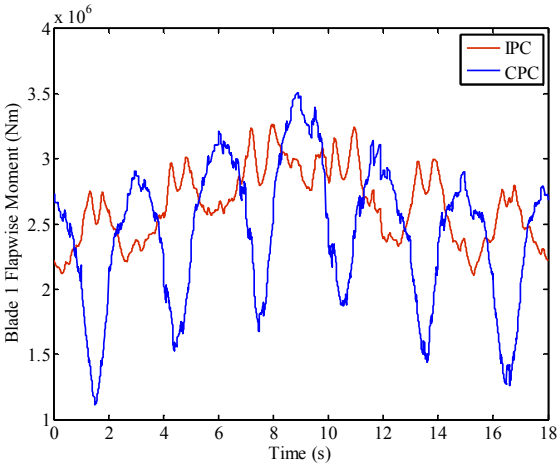

(d) The flap wise moment on the blade 1

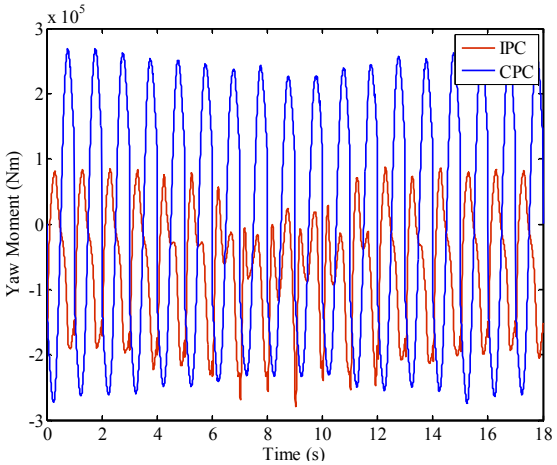

(e) The yaw moment on the tower

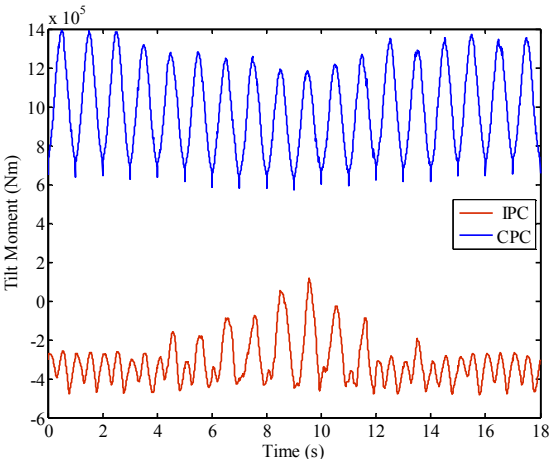

(f) The tilt moment on the tower

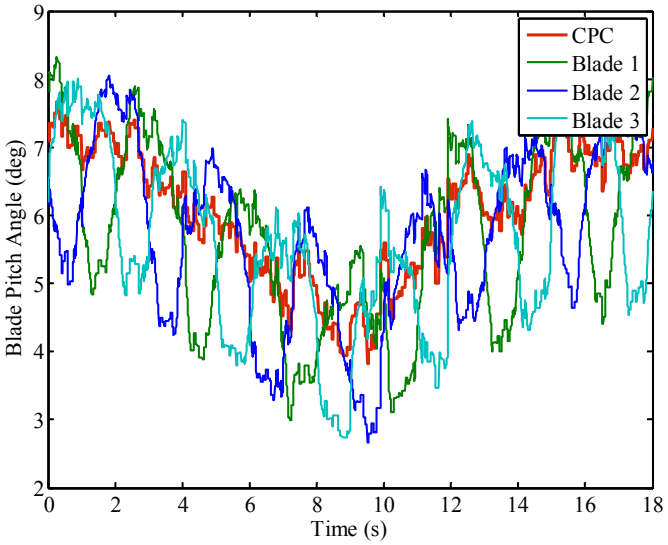

(g) The pitch angle of three Blades

Fig. 8: Control effect diagram using IPC with the turbulence wind

Figure 8g shows the pitch angle changes of the blade that meet the above-deduced IPC rules. However, the change rate of the pitch angle is so high, the frequency of the pitch action intensity increases which will put forwarded higher demands to the pitch actuator.

The other IPC based on multi-stage dynamic weight coefficient distribution of the pitch angle adjusts the pitch angle according to the dynamic weight coefficient (Dou *et al.*, 2012). The WTGS with this IPC cannot feedback controlled without load sensors. According to the above Fig. 7 and 8, the WTGS with the SNPID-IPC controller can smooth the fluctuation of the loads by sampling the blade edgewise moment and tracking feedback control. Moreover, this IPC system tracks the quick change of wind speed by means of self-learning and the adjustments of the SNPID controller. Because the wind variable in large-scale wind rotor rotating plane is severe, the WTGS with SNPID-IPC controller is obviously superior to the former system.

CONCLUSION

In this study, the blade loads and wind turbine loads are analyzed firstly and the blade edgewise moment generated by the aerodynamic force is proved to the main factor to the wind turbine torque fluctuation. To calculate the wind turbine torque and loads on the blade, a detailed dynamic aerodynamic model of the wind turbine is built based on the element theory. In addition, the influence rules of the wind turbine fluctuation caused by wind shear, tower shadow and turbulence are deduced based on this model. Moreover the IPC with SNPID controller to directly reduce the fluctuation of the edgewise moment is proposed and the SNPID controller is designed in detail. A typical 2MW WTGS is modeled and simulated with various winds. The simulation results show, the WTGS with the SNPID-IPC controller not only smoothes the wind turbine torque fluctuation and maintain the wind turbine torque at rated torque compared with the CPC WTGS, but also weakens significantly the unbalanced loads on the blade and the tower.

ACKNOWLEDGMENT

This study was supported by the Shanghai Science Foundation of China (No.08DZ1200504) and the National Natural Science Foundation of China (No. 50907040).

REFERENCES

Abdin, E.S. and W. Xu, 2000. Control design and dynamic performance analysis of a wind turbine-induction generator unit. IEEE T. Energy Conver., 15(1): 91-96.

Barlas, T., T. Hulskamp, J.W. Van and A. Mroz, 2006. Smart rotor control blades and rotor control for wind turbines. Knowledge Base Report for UpWind WP 1B3.

Bossanyi, E.A., 2003. Individual blade pitch control for load reduction. Wind Energ., 6(2): 119-128.

Bossanyi, E.A., 2005. Further load reductions with individual pitch control. Wind Energ., 8(4): 481-485.

Dou, Z.L., Z.L. Ling and X. Cai, 2011. Experimental research on virtual wind farm and wind turbine emulator system. Proc. CSEE, 31(20): 127-135.

Dou, Z.L, Z.L. Ling and X. Cai, 2012. Torque smoothing control of wind turbine generator system using individual pitch control. The 7th International Power Electronics and Motion Control Conference, Harbin, China, Jun. 2-5.

Fadaeinedjad, R., G. Moschopoulos and M. Moallem, 2009. The impact of tower shadow, yaw error and wind shears on power quality in a wind-diesel system. IEEE T. Energy Conver., 24(3): 102-111.

Geyler, M. and P. Caselitz, 2007. Individual blade pitch control design for load reduction on large wind turbines. Proceddings of the European Wind Energy Conference. Milan, Italy, May 7-10, pp: 82-86.

Hau, E., 2006. Wind Turbines: Fundamentals, Technologies, Application, Economics, Springer Verlag. Berlin Heidelberg, New York.

Hansen, M.O.L., 2008. Aerodynamics of Wind Turbines. James and James Ltd.

Haiyun, W., W. Weiqing and B. Liang, 2010. Application of individual pitch controller for flicker reduction on variable speed wind turbines. Proceedings of the 2010 Asia-Pacific Power and Energy Engineering Conference, Chengdu, China, Mar. 28-31, pp: 1-4.

Jelavic, M., V. Petrovic and N. Peric, 2008. Individual pitch control of wind turbine based on loads estimation. The 34th Annual Conference of IEEE 2008, Orlando, Florida, Nov.10-13, pp: 228-234.

Kanev, S. and T.E. Van, 2010. Wind turbine extreme gust control. Wind Energ., 13(1): 18-35.

Lackner, M.A. and G.A.M. Van Kuik, 2010. The performance of wind turbine smart rotor control approaches during extreme loads. J. Sol. Energ. Eng., 132: 011008-1-8.

Lescher, F., J.Y. Zhao and P. Borne, 2005. Robust gain scheduling controller for pitch regulated variable speed wind turbine. Stud. Informat. Control, 14(4): 299-315.

Liu, H., Y. Lin and W. Li, 2006. Study on control strategy of individual blade pitch-controlled wind turbine. Proceedings of the 6th World Congress on Intelligent Control and Automation, Dalian, China, Jun. 21-23, pp: 6489-6492.

Li, D., Z. Ye, Y. Chen and N. Bao, 2004. Load spectrum and fatigue life analysis of the blade of horizontal axis wind turbine. Eng. Mech., 27(5): 495-506.

Manwell, J.F., J.G. McGowan and A.L. Rogers, 2002. Wind Energy Explained. Wiley Online Library. New York.

Markou, H., P.B. Andersen and G.C. Larsen, 2011. Potential load reductions on megawatt turbines exposed to wakes using individual-pitch wake compensator and trailing-edge flaps. Wind Energ., 14(7): 841-857.

Selvam, K., S. Kanev, J.W. Van Wingerden, T. Van Engelen and M. Verhaegen, 2009. Feedback-feedforward individual pitch control for wind turbine load reduction. Int. J. Robust Nonlin., 19: 72-91.

Trudnowski, D. and D. LeMieux, 2002. Independent pitch control using rotor position feedback for wind-shear and gravity fatigue reduction in a wind turbine. Proceedings of the American Control Conference, Alaska, USA, May 8-10, pp: 4335-4340.

Van, E.T., 2006. Design model and load reduction assessment for multi-rotational mode individual pitch control (higher harmonics control). European Wind Energy Conference, Athens, Greece, Feb.-Mar. s27-2.

Wilson, D.G., D.E. Berg, B.R. Resor, M.F. Barone and J.C. Berg, 2009. Combined individual pitch control and active aerodynamic load controller investigation for the 5MW upwind turbine. AWEA Windpower Conference and Exhibition, Chicago, Illinois, May 4-7.

Wu, X., X. Wang, X. Xie and T. Yue, 2008. The single neuron PID controller for automotive electromagnetic clutch based on RBF NN recognition. Control and Decision Conference, Harbin, China , July 2-4, pp: 2983-2987.

Zhao, Q. and Y. Yang, 2008. Improved single neuron PID control for heavy-duty vehicle magnetorheological seat suspension. Vehicle Power and Propulsion Conference, Harbin, China, Sep. 3-5, pp: 1-3.